Size and boundary effects on the diffusive behavior of elongated colloidal particles in a strongly confined dense dispersion

Saber Naderi and Paul van der Schoot

Citation: The Journal of Chemical Physics **139**, 134909 (2013); doi: 10.1063/1.4823736
View online: http://dx.doi.org/10.1063/1.4823736
View Table of Contents: http://scitation.aip.org/content/aip/journal/jcp/139/13?ver=pdfcov
Published by the AIP Publishing

Size and boundary effects on the diffusive behavior of elongated colloidal particles in a strongly confined dense dispersion

Saber Naderi[1,2,a] and Paul van der Schoot[1,3]
[1]*Faculteit Technische Natuurkunde, Technische Universiteit Eindhoven, Postbus 513, 5600 MB Eindhoven, The Netherlands*
[2]*Dutch Polymer Institute, P.O. Box 902, 5600 AX Eindhoven, The Netherlands*
[3]*Instituut voor Theoretische Fysica, Universiteit Utrecht, Leuvenlaan 4, 3584 CE Utrecht, The Netherlands*

(Received 9 July 2013; accepted 16 September 2013; published online 3 October 2013)

In very recent experimental work, diffusive motion of individual particles in a dense columnar phase of colloidal suspension of filamentous virus particles probed by means of fluorescence video microscopy [S. Naderi, E. Pouget, P. Ballesta, P. van der Schoot, M. P. Lettinga, and E. Grelet, Phys. Rev. Lett. **111**, 037801 (2013)]. Rare events were observed in which the minority fluorescently labeled particles engage in sudden, jump-like motion along the director. The jump length distribution turned out to be biased towards a half and a full particle length. We suggest these events may be indicative of two types of particle motion, one in which particles overtake other particles in the same column and the other where a column re-equilibrates after a particle leaves a column either to enter into another column or into a void defect on the lattice. Our Brownian dynamics simulations of a quasi one-dimensional system of semi-flexible particles, subject to a Gaussian confinement potentials mimicking the effects of the self-consistent molecular field in the columnar phase, support this idea. We find that the frequency of overtaking depends on the linear fraction of particles and the steepness of the confining potential. The re-equilibration time of a column after a particle is removed from it is much shorter than the self-diffusion timescale. For the case of large system sizes and periodic boundary conditions, overtaking events do not present themselves as full-length jumps. Only if the boundary conditions are reflecting and the system is sufficiently small, full length jumps are observed in particle trajectories. The reason is that only then the amplitude of the background fluctuations is smaller than a particle length. Increasing the bending flexibility of the particles on the one hand enhances the ability of particles to overtake each other but on the other it enhances fluctuations that wash out full jumps in particle trajectories. © *2013 AIP Publishing LLC*. [http://dx.doi.org/10.1063/1.4823736]

I. INTRODUCTION

The complex phase behavior of suspensions of anisotropic colloidal particles has been studied intensively over the past few decades, experimentally, theoretically, and by means of computer simulation.[1–3] Apart from the usual isotropic phase also nematic, cholesteric, smectic, columnar, and crystalline phases have been found in a wide variety of colloidal system, including those based on inorganic rod-like and plate-like particles, stiff polymers, elongated viruses, and worm-like micelles.[4–6] Particularly attractive from a theoretical point of view are liquid crystalline dispersions of virus particles, such as the rod-like tobacco mosaic virus and the filamentous fd virus.[1,7,8] The reason is that these particles, unlike most other types of colloidal particle, are very monodisperse in length and in width. (See however the recent work of the group of Van Blaaderen on monodisperse silica rods.[9]) This makes comparison with theory and simulation a lot more straightforward than when the particles are not monodisperse. By and large, experiment, simulation, and theory agree, showing that the increasingly complex ordered phases that appear with increasing concentration of particles is due to packing effects and driven by entropy rather than enthalpy.[10]

Whilst a lot is now understood of the equilibrium structure and properties of liquid crystal phases in colloidal dispersions, remarkably little is known about kinetic processes that take place in them. It is not surprising, then, that over the past few years more emphasis is being put on unraveling *kinetic* processes in these highly congested phases.[11] It has emerged, for instance, that the diffusivity of rod-like particles along their main axis speeds up in the nematic phase as compared to that in the isotropic phase.[12] In the smectic-A phase, diffusion along the rod axis seems to be dominated by a kind of hopping-type layer-to-layer diffusion, dictated by a combination of temporary caging of particles by their immediate neighbors and the permanent self-consistent molecular field that they experience due to the presence of all other particles.[9,13,14]

Probing single particle dynamics in congested liquid crystalline dispersions has been made possible by advances in experimental techniques such as fluorescence video microscopy.[15] Indeed, by fluorescently labeling a very small portion of filamentous fd virus particles dispersed in water,

[a]m.s.naderi@tue.nl

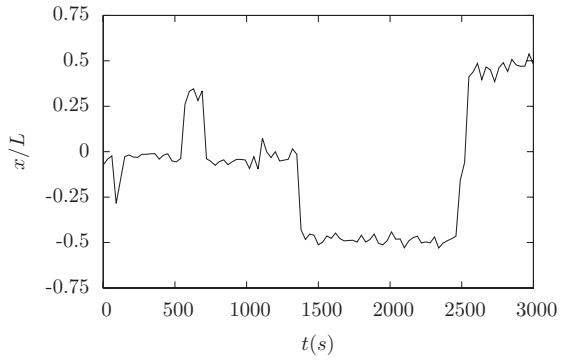

FIG. 1. Displacement x of a fluorescently labeled fd virus particle along the director in a columnar phase where concentration of fd virus particles is $c = 130$ mg/ml at a pH $= 8.2$ and ionic strength of $I = 20$ mM. The displacement is shown in unit of L the contour length of the fd virus particle and time is in units of seconds. Notice the occurrence of "full" jumps and "half" jumps of a full and half particle length. A full length jump may consist of two consecutive half jumps.[24]

Lettinga, Grelet, and collaborators[16,17] were able to probe self-diffusion in nematic and smectic-A phases, and recently also the columnar phase that appears to be hexatic rather than hexagonal.[18] By tracking individual particles they found that the particles jump between neighboring smectic layers.[14] This type of inter-layer diffusion has also been hypothesized to take place in smectic phases of thermotropic liquid crystals.[19] It has also been found in recent simulations of perfectly parallel[20] and freely rotating[21,22] hard filamentous particles.

Since the smectic phase has a layered structure, the finding of the discrete jumps is not entirely surprising. Interestingly, a similar kind of hopping-type diffusion along the main axis of the particles has also been observed in the *columnar* phase of fd virus particles, a phase in which the particles exhibit no positional ordering in this direction.[23] A typical trace is shown in Fig. 1.[24] The figure shows that almost all of the time the tracked particle jitters around some equilibrium position, to jump to a new one a few times over the course of the observations that lasted several hours. The first three jumps measure about half a particle length (that we refer to as "half jump") and the fourth one a full particle length (a "full jump").

This kind of short-time rattling punctuated by long-time jump events along the director of the columnar phase shows that the diffusion of the particles must be of non-Gaussian nature, similar to the diffusion of rod-like particles along the rod axis in the smectic-A phase, which of course is rather unexpected.[16] To investigate this, Belli *et al.*[25] performed dynamical Monte Carlo simulations of a binary mixture of perfectly aligned hard spherocylinders. The binary mixture was needed to suppress the smectic phase that for monodispersed hard rigid spherocylinders is more stable than the columnar phase. They found that exchange of particles between columns corresponds to a hopping-type diffusion in a two dimensional lattice, as expected, but that the diffusion along the columns remains classical, i.e., diffusive at short times, subdiffusive at intermediate times, and diffusive again at long times. The subdiffusive behavior at intermediate times is due to single-file diffusion; at long times it crosses over to simple diffusion due to exchange of particles between the columns.

So, no evidence of a hopping-type diffusion along the main axis of symmetry was found in these simulations. The reason for this is unclear but may be due to factors including a lacking particle flexibility, monodispersity, chirality, and soft particle-particle interactions. Due to the poly-domain structure of the columnar phase of fd virus,[18] where domains range in size from ten to a hundred particle lengths, boundary conditions should in addition become an important factor. Typically, in simulations the boundary conditions of choice are periodic ones, as in fact was in the case of the work of Belli and co-workers.[25] In the present work, we show by means of Brownian dynamics simulations on a quasi one-dimensional toy model mimicking the diffusive behavior of rod-like particles in a single column in a hexatic phase, that a plausible explanation of the full jumps may be particle overtaking events within the columns. These events can only be observed if the inherent fluctuations associated with the in-line diffusion in the columns are sufficiently suppressed. This requires small system sizes *and* reflecting boundary conditions. We put forward that the observed full jumps are in essence a result of the poly-domain structure of the columnar phase.

The half jumps we hypothesize to be due to particles moving out of a column either to a neighboring column or to a defect, leading to very fast relaxation of the remaining of the particles in that column due to the large pressure. In our simulations, we test this by removing a single particle from the column and following the trajectories of the neighboring particles. The time dependence of the re-equilibration that we find agrees well with a simple estimate based on equating the in-line pressure (a force) to the friction a particle experiences. We find that the timescale associated with the re-equilibration is very short on the time scale of the short-time self-diffusivity of the particles, in agreement with observations on fd virus.[23]

The structure of the remainder of this paper is as follows. In Sec. II we first describe the simulation model and the way that we analyze the simulation data. In the model we focus attention on diffusive processes in a single column subject to a Gaussian confining potential. The confining potential mimics the effect of the self-consistent molecular field imposed by particles in the other columns. In Sec. III we discuss our simulation results for the mean-square displacement of rigid rod-like particles. In Sec. IV we present our simulation results for correlation functions as a function of the strength of the confining potential and the linear fraction of the particles that we model as strings of beads. Section V discusses the relaxation of the particles in a column following the removal of a single particle from it, again as a function of linear density in the limit of strong confinement. Next, in Sec. VI, we investigate the impact of bending flexibility in particular on the mean-square displacements and the Van Hove correlators of the particles. We end the paper with a discussion and conclusions in Sec. VII.

II. MODEL AND SIMULATIONS

We perform Brownian dynamics simulations on systems containing N elongated particles, each consisting of a linear

array of $n = 5$ beads. Within each chain-like particle, adjacent beads are bound to each other via a harmonic bond potential of the form $U_{bond}(r) = k_b(r - l_b)^2$, and each three neighboring beads are linked by a harmonic bending potential $U_{bend}(\theta) = k_a(\theta - \pi)^2$, where r is the distance between the centers of mass of pairs of bead, $l_b = 1.2\sigma$ is the equilibrium bond length with σ the size (diameter) of the beads and θ the angle formed by the two bonds that connect the three beads to each other. Furthermore, k_b and k_a are the strengths of the bond and bend potentials, respectively. In all our simulations, we choose a large value for the strength of the bond potential, $k_b = 50\ k_BT/\sigma^2$, to ensure an essentially fixed bond length during the simulations. The relation between k_a and the persistence length L_p of each particle is $L_p = 2\ k_a l_b/k_BT$,[26,27] at least in the limit where $n \to \infty$ and $k_b l_b^2/k_BT \gg 1$, where k_BT is the thermal energy with k_B Boltzmann's constant and T is the absolute temperature. In our simulations we focus attention on ratios $L/L_p = 0.066$–4 of the contour length $L = (n - 1) \times l_b$ of our particles in the stiff bond limit that we are considering and persistence length of the particles L_p. This allows us to investigate the effect of particle flexibility on the kinetics.

All beads that are not direct neighbors in a chain interact with each other through the repulsive part of a shifted Lennard-Jones potential,

$$U_{ij}(r) = \begin{cases} 4\epsilon((\frac{\sigma}{r})^{12} - (\frac{\sigma}{r})^6 + \frac{1}{4}) & \text{if } r \le 2^{\frac{1}{6}}\sigma \\ 0 & \text{if } r > 2^{\frac{1}{6}}\sigma \end{cases}, \qquad (1)$$

where $\epsilon \equiv k_BT$ is the strength of the interaction potential, which in our simulations is equal to the thermal energy k_BT, and r is again the center-to-center distance between the beads. This potential mimics the soft electrostatic repulsion that acts between the charge-stabilized fd virus particles.[18,23]

In order to mimic the self-consistent molecular field in the columnar phase, a harmonic external potential is applied to all beads,

$$U_{ext} = k_{ext}(y^2 + z^2), \qquad (2)$$

where k_{ext} is the strength of confining potential and y and z are the Cartesian coordinates perpendicular to the main axis (the x axis) of the confining potential (see Fig. 2). Note that this external potential influences the apparent flexibility of particles and introduces another length scale other than the persistence length, related to the strength of the confining potential and the persistence length.[28]

The strength of the confining potential must somehow be linked to the concentration of the particles in the columnar phase. In principle, the relation between k_{ext} and particle density (or packing fraction) can be estimated, e.g., from the simulation results of Belli and co-workers.[25] This is possible because the radial density distribution, the distribution of particles in the direction perpendicular to the director of the particles, is proportional to the Boltzmann factor of the self-consistent molecular field.[16] Ignoring the fact that the simulations involve binary mixtures of long and short spherocylinders with aspect ratios $L/\Delta = 2.1$ and 1.0, where L and Δ are the length and diameter of a cylindrical body capped by two hemispheres with diameter Δ, Belli *et al.* found that for

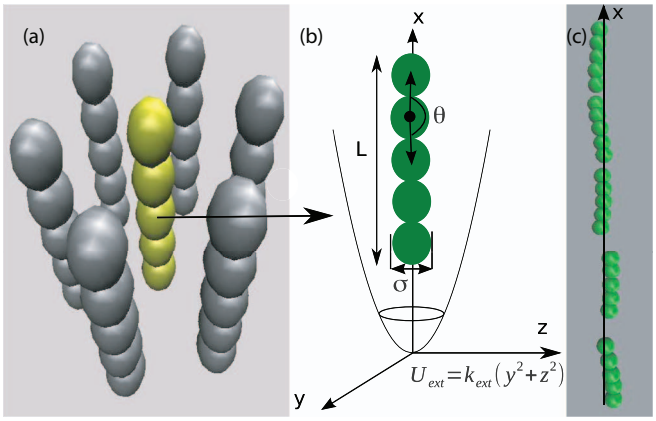

FIG. 2. (a) Schematic representation of a particle in a hexagonal columnar phase. (b) Each particle in our simulations consists of five beads connected by strong harmonic springs as well as harmonic bending potentials between pairs of bonds. An external harmonic confining potential is applied to all beads mimicking the self-consistent molecular field that particles in a column of the columnar phase experience due to presence of particles in other columns. (c) Snapshot of a simulation with $N = 5$ particles, linear fraction of particles $\psi = 0.8$, and the strength of the confining potential $k_{ext} = 7\ k_BT/\sigma^2$.

volume fractions $\eta = 0.535$, 0.563, and 0.580, the strength of the external potential applied to each rod is 30.9 (25.6), 55.6 (44.5), and 69.3 (56.5) k_BT/Δ^2 for the longer (shorter) rods, respectively.[29] Here the external potential applies to rods, not segments. To obtain the strength of the external potential that is applied to beads, we divide these values by the number of beads in each particle, which in our simulations is $n = 5$. This gives us for the strength of the confining potential applied on each bead $k_{ext} = 6.2$, 11.1, and 13.9 k_BT/σ^2 for the three concentrations quoted. Note that in obtaining these values we ignored the fact that the aspect ratio of particles in these simulations is different from those in ours. In our simulations, we mostly apply smaller values for the strength of the external potential in the range $k_{ext} = 2.0$–$3.0 k_BT/\sigma^2$. This helps us observe the overtaking events more often and to obtain better statistics. For the special case where we focus on single-file diffusion, in which mutual passage of particles is not allowed, much larger values of the confining potential strength are used, $k_{ext} = 5.0$–$20.0\ k_BT/\sigma^2$. This ensures that overtaking events do not occur during these simulations.

We used LAMMPS molecular dynamics package[30] for all our simulations. To implement the external potential of Eq. (2), we add a custom potential to the LAMMPS code. Our simulations are performed with a time step of $5 \times 10^{-3}\ t^*$, where t^* is the unit of time, set by the self-diffusion constant of a single bead $D_b = \sigma^2/t^*$. The self-diffusion constant of an elongated particle made up of n beads reads $D = D_b/n$, at least in the free-draining limit in which we are operating.[31] Initially, at time $t = 0$, the particles are positioned equidistantly on a line with a given linear fraction ψ. To avoid a bias of our simulation results towards the initial state, we discard the first $1.0t^*$ of the simulation data. This is sufficient because in most of our simulations the linear fraction is close to unity, which means that the internal pressure is high and the system reaches equilibrium very quickly. To investigate the effect of the boundaries on the dynamics of the particles

periodic and reflecting boundary conditions are applied in the direction of the main axis of the confining potential. Reflecting boundary conditions are imposed by putting two fixed walls at $x = -0.5\sigma$ and $x = \lambda + 0.5\sigma$, where λ is the length of the simulation box along the main axis (the x axis). These walls interact with beads through the repulsive part of a shifted Lennard-Jones potential,

$$U_{wall}(\Delta x) = \begin{cases} 4\epsilon((\frac{\sigma}{\Delta x})^{12} - (\frac{\sigma}{\Delta x})^{6} + \frac{1}{4}) & \text{if } \Delta x \leq 2^{\frac{1}{6}}\sigma \\ 0 & \text{if } \Delta x > 2^{\frac{1}{6}}\sigma \end{cases}, \tag{3}$$

where Δx is the shortest distance between the center of a bead and the wall.

We analyze the structure and diffusion of the particles in the quasi one-dimensional system by calculating the mean-square displacement of the particles $w(t)$, the self-part of the Van Hove correlation function G_s,[32] the pair correlation function g_2,[33] and the trajectory of particles for different values of (i) the linear fraction ψ, (ii) the strength of the external potential k_{ext}, and (iii) the bending flexibility k_a. In order to quantitatively investigate the hopping-type diffusion of particles in our simulations, the probability of finding a particle at a distance x after an interval of time t from its position along the main axis of the confining potential at time $t_0 \equiv 0$,[32]

$$G_s(x,t) = \frac{1}{N}\left\langle \sum_{i=1}^{N} \delta[x + x_i(0) - x_i(t)] \right\rangle, \tag{4}$$

which is the self part of Van Hove function, where N is the number of particles, $x_i(t)$ is the position of the ith particle at time t, and the angular brackets mean ensemble average. For particles diffusing in a dilute gas, where the particles do not interact with each other, G_s is a Gaussian function of the coordinate x.[33] As the concentration of particles increases and particle-particle interactions become important, the self part of Van Hove function starts to deviate from a Gaussian.[34] This is because at high packing fractions the motion of particles is affected by the presence of neighboring particles (due to the caging effect) and this induces dynamical heterogeneities in the system.[13]

In systems where particles need to overcome a high free energy barrier to diffuse around, e.g., due to the presence of a self-consistent molecular field such as in the case of a smectic phase,[13] the motion of the particles is a combination of rattling- and hopping-type diffusion. This means that particles are mostly rattling around minimum energy positions and after some time they hop to another one. For the case that particles hop with a certain hopping length, the self part of the Van Hove function is not a Gaussian function and peaks appear for certain values of x that are multiples of the hopping length[35] (see also below).

The dynamics of particles in a congested system is arguably directly connected to its local (microscopic) structure. For instance, the hopping-type diffusion observed in the smectic-A phase is due to periodic particle density variations along the director. Therefore, the study of the structural functions such as particle density and pair correlation function helps us understand the dynamics. The particle density is a measure of the density variations in a system and the pair correlation function is a measure of the density variations as a function of the distance from a particle. In one dimension, the single-particle density may be written,[36]

$$n(x) = \left\langle \sum_{i=1}^{N} \delta[x - x_i] \right\rangle, \tag{5}$$

where the angular brackets imply an ensemble average and $\delta(x)$ is the Dirac delta function. For homogeneous and translationally invariant one-dimensional systems the pair correlation function is given by,[33]

$$g_2(x) = \frac{\lambda}{N^2}\left\langle \sum_{j\neq i=1}^{N} \delta[x + x_i - x_j] \right\rangle, \tag{6}$$

where λ is the length of the system, and $N \gg 1$ is the total number of particles.

It can be shown that the single-particle density near a reflecting boundary behaves like the pair correlation function of the same system in the bulk, i.e., away from the boundaries.[37] So, conversely, the structure of a system near the boundaries can be deduced from the pair correlation function, which for a one-dimensional system of hard rods with linear fraction ψ reads[38]

$$g_2(x) = \frac{1}{\psi}\sum_{k=1}^{\infty} \Theta\left(\frac{x}{L} - k\right)\left(\frac{\psi}{1-\psi}\right)^{k} \frac{(\frac{x}{L} - k)^{k-1}}{(k-1)!} \times \exp\left[-\frac{\psi}{1-\psi}(\frac{x}{L} - k)\right], \tag{7}$$

where x is the center-to-center distance between particles, L is the particle length, and $\Theta(x)$ is the Heaviside step function with $\Theta(x) = 0$ or 1 for $x < 0$ or $x \geq 0$, respectively. In our simulations, Eq. (7) should apply to the situations of extreme confinement where particles cannot overtake. When the strength of the confining potential, k_{ext}, is not large enough to prevent particles from overtaking each other, deviations from this relation are expected.

III. RIGID RODS: MEAN-SQUARE DISPLACEMENT

For a finite-size, truly one-dimensional system in which mutual overtaking of particles is not allowed, three diffusion regimes characterize the mean-square displacement $w(t)$.[39] The first regime corresponds to the short-time Fickian diffusion regime, where a test particle does not feel the presence of the other particle. In the second regime, called the single-file diffusion (SFD) regime, diffusion of particles is suppressed by the others and the mean-square displacement exhibits subdiffusive behavior. At times $t \gg t_N$, where t_N is a crossover time that depends on the system size λ and the linear fraction of particles ψ, the mean-square displacement, which is also a measure of fluctuations in the position of particles, reaches either a plateau value (for the case of reflecting boundary conditions)[39,40] or a Fickian diffusive regime in which the entire system diffuses, that is, its center of mass (for the case of periodic boundary conditions).[39] Our simulation results for the case of highly confined rigid particles (with $L/L_p = 0.067$) are shown in Fig. 3 for systems of $N = 5$ particles with periodic and reflecting boundary conditions. For the latter, the

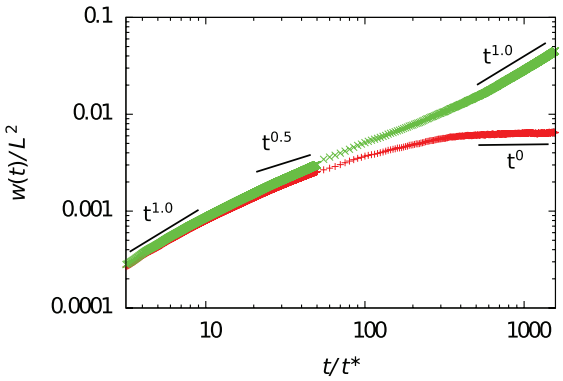

FIG. 3. Dimensionless mean-square displacement, $w(t)/L^2$, as a function of dimensionless time, t/t^*, for a system of $N = 5$ particles with reflecting (red plus signs) or periodic (green crosses) boundary conditions, in a cylindrically symmetric harmonic confining potential. Here, L is the contour length of particles consisting each of five beads of diameter σ, and t^* is the simulation time unit $t^* = \sigma^2/D_b$ where D_b is the self-diffusion constant of a single bead. The linear fraction of particles in our quasi one-dimensional system is $\psi = 0.6$ and the strength of the Gaussian confining potential is $k_{ext} = 7\, k_BT/\sigma^2$, where k_BT is the thermal energy. Lines indicate the three diffusion regimes where in the first regime, at short times, particles do not feel each other's presence and $w(t) \propto t$. In the second regime, the motion of particles is affected by the fact that they cannot pass each other, giving a subdiffusive $w(t) \propto t^{1/2}$ typical of single-file diffusion,[41] while in the third regime $w(t)$ reaches a plateau value (for the case of reflecting boundaries) or the entire system collectively moves as a single free particle and again $w(t) \propto t$ (for the case of periodic boundaries).

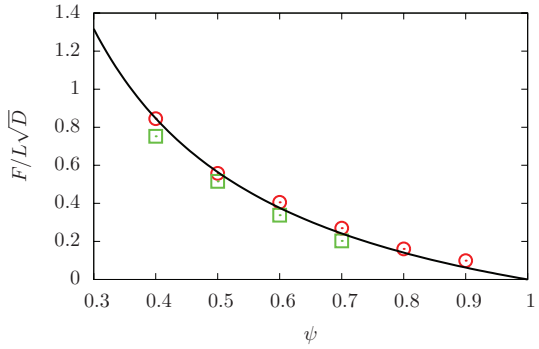

FIG. 4. Single-file diffusion mobility F as a function of linear fraction ψ. Circles are obtained from the simulations where particles are strongly confined to a line by a confining potential with harmonic spring constant $k_{ext} = 10\, k_BT/\sigma^2$, obtained by fitting mean-square displacement to $w(t) = 2Dt/(1 + (D/F)t^{1/2})$, where D is the single-particle diffusion constant.[43] Squares are resulted from the same simulations by calculating the structure factor and substituting it in Eq. (8). The solid line is a theoretical prediction valid for a truly one-dimensional hard-rod fluids.[41] It is due to finite size of our systems that the simulation results obtained from Eq. (8) slightly underestimate the theoretical prediction.

fluctuations in the position of particles is suppressed at long times by the small system size and boundary effects. This is because the maximum available "volume" for particles to diffuse is limited by the system size.

For an infinitely large system of identical particles with arbitrary interaction potential and finite-range correlation length between particles, the third regime disappears because the maximum free space available for particles is in principle infinitely large. The mean-square displacement in the second regime follows the expression $w(t) = 2Ft^{1/2}$, where F is the single-file diffusion mobility, given by[42]

$$F = 1/\rho\sqrt{DS(0)/\pi}, \tag{8}$$

with D the self-diffusion constant, ρ the particle number density, and $S(0)$ the structure factor, $S(q)$, at the wave vector $q = 0$. For a one-dimensional Tonks gas this gives $F = [L(1-\psi)/\psi]\sqrt{D/\pi}$, where L is the particle length and $\psi = \rho L$ is the linear fraction of particles.[41] The crossover time t_{SFD} from the first to the second regime is given by $t_{SFD} = [L(1/\psi - 1)]^2/2D$. Our simulations confirm this. Shown in Fig. 4 is the single-file mobility as a function of linear fraction ψ for simulations with a large value for the strength of confining potential $k_{ext} = 10\, k_BT/\sigma^2$. For this value of the confining potential the particles do not overtake each other during the simulations and our system behaves like a one-dimensional gas.

By decreasing the strength of confining potential, the constraint that does not allow particles to overtake each other is relaxed and a crossover in the mean-square displacement from subdiffusive scaling (in the SFD regime) to a diffusive one (Fickian regime) occurs for long times.[44] The crossover time is related to an overtaking time t_O that measures the average time for two particles to overtake each other.[45] In our model, this overtaking time depends on the strength of the confining potential and the linear fraction of particles. We come back to this below. For an infinitely large system and $t_O \gg t_{SFD}$ the SFD regime is reached by the collection of particles between overtaking events, and the average mean-square displacement of the particles scales as $w(t_O) \sim Ft_O^{1/2}$.[45] Therefore, the average overtaking length, that is, the average displacement of a particle after an overtaking event, $\sqrt{w(t_O)}$, in this case is not necessarily a multiple of the particle length and can be any number depending on F and t_O.

This contrasts with the experimental observations on *fd* virus particles in the columnar phase that discrete jump events are found in the trajectory of particles.[23] This is an indication that the poly-domain structure of the columnar phase and the finite size of the columns might play an important role in the dynamics of particles in this phase. The domain size in the columnar phase can be roughly estimated from the optical texture of this phase by polarizing microscopy. The estimated size of each domain is about 10–100 μm, which is about 10–100 times the fd virus particle length (0.88 μm).[18]

Here, we argue how the column size could affect the particle dynamics. As mentioned earlier, for small system sizes the fluctuation in the position of particles (the square root of the mean-square displacement) reaches a plateau value, see Fig. 3. For sufficiently small system sizes with reflecting boundary conditions and sufficiently large linear fractions, these fluctuations are actually much smaller than the particle size. In this case, the average overtaking length approximately equals a particle length because in an overtaking event particles that are rattling around their initial positions suddenly exchange positions.

To illustrate the importance of system size, trajectories of particles in a large system with periodic boundary conditions and a small system with reflecting boundary conditions are shown in Fig. 5. The latter is similar to the experimental traces

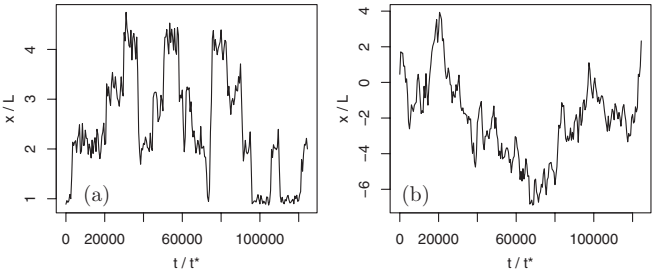

FIG. 5. Position, x, of particles normalized to their contour length, L, as a function of dimensionless time t/t^* (a) small system for which background fluctuations in the position of particles, $w(t)$, is suppressed by the system size ($N = 10$ particles) and reflecting boundary conditions. (b) Large system with $N = 200$ particles and periodic boundary conditions. In both simulations, the strength of the confining potential is $k_{ext} = 3\ k_BT/\sigma^2$ and the linear fraction of particles is $\psi = 0.9$.

shown in Fig. 1. This rattling- and hopping-type motion is also reminiscent of the diffusion of particles along the director in a smectic-A phase where particles hop between smectic layers. This type of motion in the smectic-A phase leads to appearance of peaks in the self part of the Van Hove function. So, we would expect to see peaks in the self part of the Van Hove function G_s for the case of a small system with reflecting boundary conditions, at least for confining potentials that are not so steep that overtaking events do not occur.

IV. RIGID RODS: CORRELATION FUNCTIONS

In order to test the idea that in small systems the Van Hove function G_s exhibits correlation peaks, we calculated G_s for systems with periodic and reflecting boundary conditions. As expected, for the case of a small system with reflecting boundary conditions, peaks appear on multiples of the particle length; see Fig. 6(a). For the case of a relatively large system ($N = 200$) with periodic boundary conditions, where the effect of overtaking events on the trajectories is washed out by the fluctuations, no peaks appear on multiples of the particle length in the self part of the Van Hove function (see Fig. 6(b)). In this case, G_s is a superposition of Gaussian functions corresponding to the short-, intermediate-, and long-time diffusion of particles. The time scales involved are the (short-

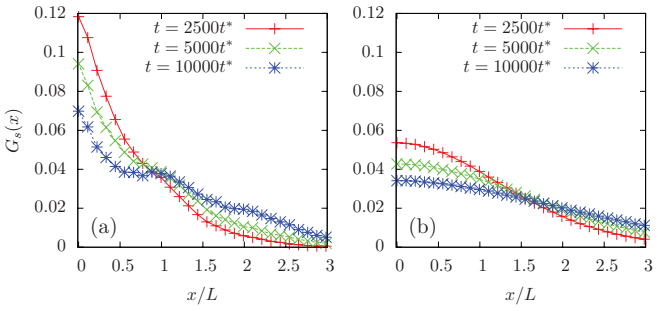

FIG. 6. The self part of the Van Hove function G_s as a function of the scaled coordinate x/L along the main axis of the system after time intervals $t = 2500t^*$, $5000t^*$, and $10000t^*$. (a) $N = 10$ particles and reflecting boundary conditions. (b) $N = 200$ particles and periodic boundary conditions. Here, the linear fraction of particles is $\psi = 0.9$, the strength of the confining potential is $k_{ext} = 3\ k_BT/\sigma^2$ and L is the particle length.

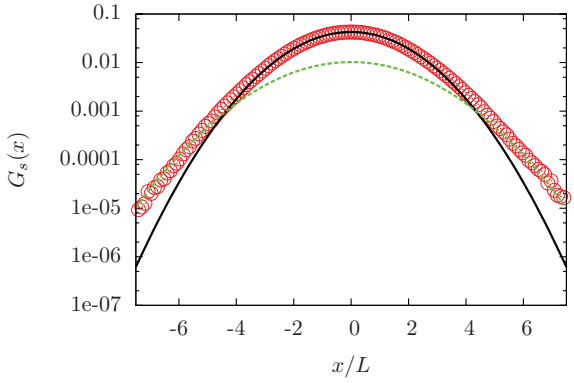

FIG. 7. Self part of the Van Hove function G_s as a function of the dimensionless displacement x/L for a system of $N = 200$ particles with linear density $\psi = 0.9$ and subject to a harmonic confining potential $k_{ext} = 3\ k_BT/\sigma^2$ after a time interval $t = 2500t^*$. Periodic boundary conditions are applied in this simulation. L is the length of a particle. The black solid line is a Gaussian fit to data points around the origin ($x^2/L^2 < 5$) which refers to SFD and the green dashed line is a Gaussian fit to the tail of the distribution ($25 < x^2/L^2 < 64$).

time) self-diffusion, (intermediate-time) single-file diffusion, and (long-time) hopping-type diffusion time scales.

The effect of these different time scales on G_s can be seen in Fig. 7 where two Gaussian functions are fitted to the head and the tail of the Van Hove function G_s. These two functions correspond to the intermediate and long time scales. The one corresponding to the short time scales cannot be calculated from this figure because there are not enough data points at the head of the G_s; the frequency at which data are recorded is not high enough. Our results are similar to what Belli *et al.*[25] find for the longitudinal component of the self part of the Van Hove function of a columnar phase of bidisperse parallel spherocylinders with periodic boundary conditions. (Note that the mechanism of hopping-type diffusion along the main axis is slightly different from ours since in their simulations inter-column jumps occur.) Therefore, it may well be so that it is because of the periodic boundary conditions that Belli *et al.* do not find rattling- and hopping-type diffusion along the director in their simulations.

The effect of boundary conditions becomes more important when the system gets smaller. This can be understood by considering the fact that for a small system the fraction of particles that feel the presence of the boundaries increases. Shown in Fig. 8(a) is the self part of the Van Hove function G_s for simulations with reflecting boundary conditions and three system sizes ($N = 5$, 10, and 50). For the smaller systems there is a peak in the G_s for a displacement $x/L = 1$. For the system with $N = 50$ particles this peak is washed out because there are many particles in the middle of the system of which the motion is not affected by the boundaries. This shows that there must be a certain system size at which most of the particles do not feel the presence of the boundaries. This certain system size depends on the linear fraction of particles because the spatial correlation length is determined by the linear fraction. The effect of linear fraction on the self part of the Van Hove function for a system of $N = 10$ particles is shown in Fig. 8(b). As the linear fraction increases the peak located at displacement $x/L = 1$ becomes more prominent,

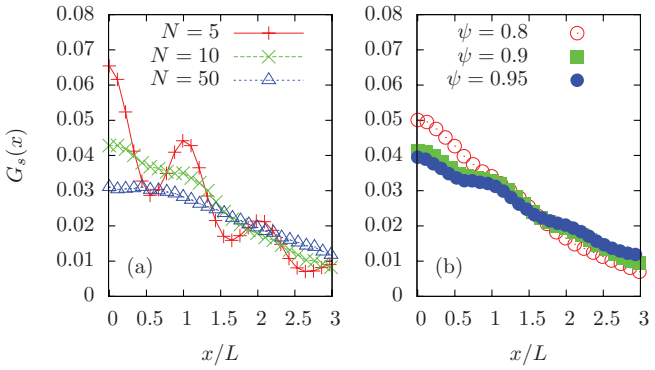

FIG. 8. Self part of the Van Hove function $G_s(x)$ as a function of dimensionless displacement x/L for time $t = 5000t^*$ obtained from simulations in which the strength of the confining potential is $k_{ext} = 2\ k_BT/\sigma^2$ and the boundary conditions are reflecting. (a) Result for three system sizes with $N = 5$, 10, and 50 particles and a fixed linear fraction of particles $\psi = 0.9$. (b) Result for three values of linear fraction $\psi = 0.8$, 0.9, and 0.95 with the number of particles fixed to $N = 10$.

which means that more particles are making jumps that are not washed out by the fluctuations. This is not surprising because, as mentioned earlier, by increasing the linear fraction the spatial correlation length increases and this means that the motion of more particles is affected by the boundaries.

To better understand this we can calculate other structural descriptions such as the particle density and pair correlation functions. As mentioned earlier, the behavior of the particle density function near a reflecting boundary is proportional to that of the pair correlation function of the same system in the bulk (see Fig. 9). The pair correlation function for a one-dimensional system of hard rods with linear fraction ψ is given by Eq. (7). This pair correlation function is an oscillating function of the center-to-center distance between particles, x, with a decaying envelope the decay length of which

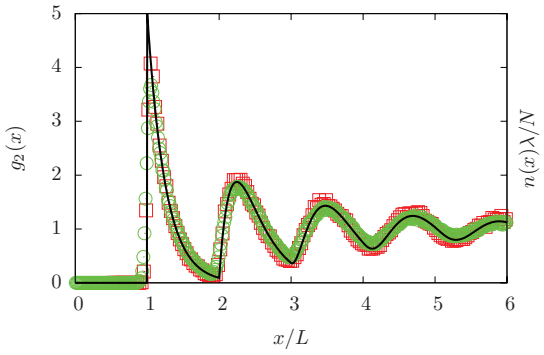

FIG. 9. Green circles: pair correlation function $g_2(x)$ as a function of dimensionless displacement x/L of particles in a quasi one-dimensional system with $N = 50$ particles, linear fraction of $\psi = 0.8$, strength of the confining potential of $k_{ext} = 20\ k_BT/\sigma^2$, and periodic boundary conditions. L is the particle length. Red squares: the linear particle density $n(x)$ relative to the average value N/λ near the walls for a system with $N = 50$ particles, $\psi = 0.8$, $k_{ext} = 20\ k_BT/\sigma^2$, and reflecting boundary condition. λ is the system length. The black solid line is the theoretical prediction for the pair correlation function of a truly one-dimensional system of hard rods (see Eq. (7)). The displacement x is either the center-to-center distance between two particles (for the case of the pair correlation functions) or the distance from center of a particle to one of the reflecting boundaries (for the case of the particle density).

depends on the linear fraction ψ. At low linear fractions, this function decays very rapidly and it has only one peak, but as the linear fraction increases, more peaks appear near $x = 0$ (i.e., near the walls in the case of a system with reflecting boundaries) meaning that the position of particles is more restricted close to the reference particle (or close to the walls). As mentioned in the Introduction, Eq. (7) is valid for a truly one-dimensional system but for a system where the strength of the confining potential k_{ext} is not sufficiently large to prevent particles from overtaking, the pair correlation function deviates from Eq. (7). In our simulations this deviation is not large because k_{ext} is relatively large and the overtaking events occur rarely, therefore the periodic structure near the boundaries survives.

This periodic structure is reminiscent of the periodic structure of the smectic phase and induces a smectic-like molecular background field on the particles. The effect of this molecular field on the motion of particles is important when the system is sufficiently small so that the decay length of the pair correlation function is comparable with the system size, in particular if the confinement is not infinite and the particles are able to overtake each other. Therefore, in order to sensibly analyze the dynamics of particles of very dense phases such as the columnar phase with a poly-domain structure in terms of bulk dynamics, care needs to be taken to make certain that the size of the domains is much larger than the spatial correlation length.

V. HALF JUMPS

In Secs. III and IV we have shown that a possible explanation of the full jumps observed in the columnar phase of fd virus particles may be due to particle overtaking events.[23] Also, we found that the effect of system size and boundary is important because these effects may suppress fluctuations in the motion of particles and lead to formation of quasi periodic free energy barriers near the boundaries. By overcoming these free energy barriers particles can overtake each other and make full jumps. In this section, we test our hypothesis for the half jumps presented in the Introduction. According to this hypothesis, the half jumps occur due to particles moving out of a column to a neighboring column or to a defect. This leads to a very fast relaxation of the remaining particles in that column because of the large pressure in it if the linear densities are large.

Here, we test our hypothesis by removing a single particle from the system at time t_r and following the trajectory of the neighboring particles at time $t > t_r$. Removing a particle from the system creates a gap that the two neighbors of the removed particle will fill. The distance between the two neighboring particles is measured in our simulations as a function of time. For each set of parameters, we perform 100 simulations with different random generator seeds to have sufficient statistics to find the average distance between the two neighbors at times $t > t_r$. We find that after removal of the particle, the two neighbors start to move towards each other and the distance between the particles decreases exponentially until they reach an equilibrium distance after a certain amount of time (see also the supplementary material).[46] Just after the

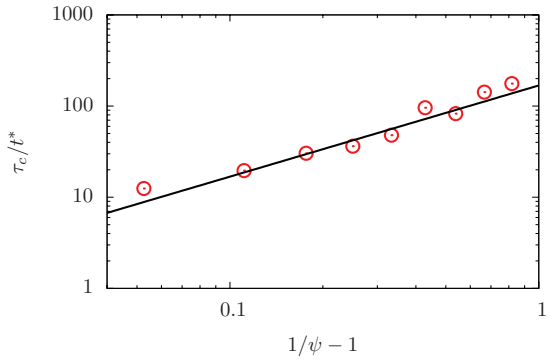

FIG. 10. The characteristic half-jump time τ_c (discussed in the main text) as a function of the linear packing fraction ψ. The data points are calculated from simulations with a strong confining potential, $k_{ext} = 10\ k_BT/\sigma^2$. The number of particles and their bending flexibilities are $N = 200$ and $k_a = 30\ k_BT$, respectively. The black solid line is the theoretical prediction, Eq. (10).[47]

particle is removed, the distance between the two neighbors is roughly twice the particle length but after a while it reaches an equilibrium value, which is, at high enough linear fractions, about the particle length. This shows that, on average, each neighbor moves a distance, which is equal to half a particle length.

From the exponential decay of the average distance between the two particles, $d_{ave}(t)$, one can calculate the average time after which the two particles fill the gap. This is also an interesting quantity because the time-scale of the half-jumps seen in the experiments is exceedingly short compared to the diffusion time-scale.[23] By fitting an exponential function of the form $d_{ave}(t) = d_0 \exp(-t/\tau_c) + d_{eq}$ to our simulation data for each value of the linear fraction, we obtain the characteristic time (τ_c) that is a measure of the time to fill the gap (see Fig. 10). It scales as $(1 - \psi)/\psi$.

In order to understand this, we derive a relation between τ_c and ψ by using the relation between the internal pressure of a Tonks gas and the linear fraction.[47] If a particle is removed from the system, the two neighboring particles are pushed towards each other by the remaining particles due to the in-line pressure. The force that drives the two neighbors to move towards each other is related to the internal pressure of a Tonks gas, given by[48]

$$\beta\Pi = \frac{\rho}{1-\psi}, \tag{9}$$

where $\beta = 1/k_BT$, Π is the internal pressure of the Tonks gas, and ρ is the number density $\rho = \psi/L$ with L being the particle length. Recall that our particles behave like a Tonks gas for large values of the confining potential. Since the system is presumed to be in the overdamped regime, the driving force is equal to the frictional force and this gives $\Pi = \gamma v$, where γ is the friction constant and v is the velocity of the particles. The length x that a particle travels after a certain amount of time t is given by $x = vt$, by replacing x with L and t with τ_c and substituting v from the above equations, we have

$$\tau_c = L^2\beta\gamma(1/\psi - 1) = \tau_D(1/\psi - 1), \tag{10}$$

where $\tau_D = L^2/D$ is the single-particle diffusion time. This equation shows that the process of filling the gap at high linear fractions happens much faster than the single particle diffusion in particular if $\psi \to 1$. In Fig. 10, a double logarithmic plot of τ_c as a function of $1/\psi - 1$ is shown. The solid line in this graph comes from the above theory, Eq. (10), which is in good agreement with the simulation results. Note that there are no adjustable parameters.

VI. EFFECT OF BENDING FLEXIBILITY

In Secs. III–V we have discussed the influence of the system size and boundaries on the dynamics of particles. We found that the formation of quasi-periodic structures near the boundaries induced by the presence of the hard walls leads to the appearance of peaks in the Van Hove function. These peaks become sharper with increasing linear fraction. This means that at higher linear fractions more overtaking events take place that are not washed out by the background fluctuations. Another factor that can affect the overtaking events and the sharpness of the peaks in the Van Hove function is the bending flexibility of particles. The reason why bending flexibility is interesting for us is that fd virus is a semi-flexible particle and that this can affect the structure of the phases formed by these particles as well as the dynamics of particles in these phases.[49]

In order to study the effect of bending flexibility on the dynamics of particles, we performed simulations with different values of the strength of the particle bending flexibility and measured the self part of the Van Hove function. Shown in Fig. 11(a) is the self part of the Van Hove function after a time interval $t = 5000t^*$ for three values of the strength of the bending flexibility corresponding to values of $L/L_P = 4.0$, 1.0, and 0.5 with increasing bending stiffness. For the case of the most flexible particles ($L/L_P = 4.0$), no peak appears for $x = L$, which means that background fluctuations are not small enough causing the overtaking events to be washed out by these fluctuations. The reason why fluctuations are bigger than for the case of stiff particles is that flexible particles can make use of their bending flexibility to reduce the internal pressure by partially lying on top of each other; this decreases the effective linear fraction and increases the magnitude of fluctuations.

As the bending stiffness is increased, partially lying on each other costs more energy for particles and therefore it is not energetically favorable to reduce the internal pressure by doing that. This is why we see shoulders appearing on $x = L$ in the $G_s(x)$ for increasing particle stiffness. So, the transition point from where there is no peak on the self part of the Van Hove function to where peaks appear in this function is determined by the energy cost for particles lying on each other. This energy cost does not only depend on the bending flexibility but also on the strength of the external potential.

In order to investigate the effect of the strength of the external potential k_{ext} on the overtaking events we performed simulations with different values of k_{ext} while keeping bending flexibility fixed $k_a = 6\ k_BT$ corresponding to $L/L_P = 1/3$, which is close to that of wild-type fd virus and is much larger

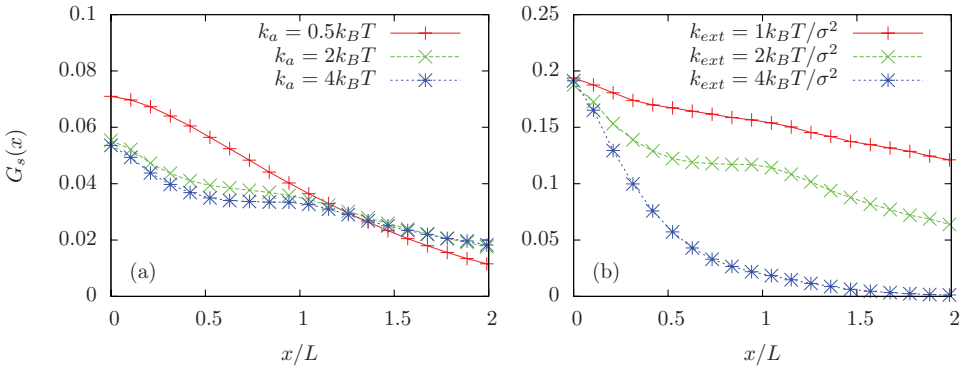

FIG. 11. Self part of the Van Hove function $G_s(x, t = 5000t^*)$ as a function of the dimensionless displacement x/L obtained from simulations with $N = 10$ number of particles and linear fraction of $\psi = 0.95$. (a) Result for three values of bending flexibility $k_a = 0.5\ k_BT$ (corresponding to a length to persistent length ratio of $L/L_P = 4$), $k_a = 2\ k_BT$ ($L/L_P = 1$), and $k_a = 4\ k_BT$ ($L/L_P = 0.5$) with a fixed value for the strength of the confining potential $k_{ext} = 2\ k_BT/\sigma^2$. (b) Simulation results for three values of the strength of the confining potential $k_{ext} = 1\ k_BT/\sigma^2$, $k_{ext} = 2\ k_BT/\sigma^2$, and $k_{ext} = 4\ k_BT/\sigma^2$ with a fixed value of the bending flexibility $k_a = 6\ k_BT$ ($L/L_P = 1/3$). Vertical axis is rescaled to get the same value at $x/L = 0$.

than $L/L_P = 0.067$ discussed in Secs. III–V. From these simulations we obtained the self part of the Van Hove function after the time interval of $t = 5000t^*$. As can be seen in Fig. 11(b) for the smallest value of k_{ext} no peak appears for $x = L$. This is again because particles are able to partially lie on top of each other and reduce the internal pressure of the system by rotating away from the center of the column giving rise to a lower effective packing fraction. This again enhances background fluctuations that wash out the effect of overtaking events. For the slightly larger value of the strength of the external potential $k_{ext} = 2\ k_BT/\sigma^2$ a shoulder appears on $x = L$ but at $k_{ext} = 4\ k_BT/\sigma^2$ the shoulder disappears again. This is because in this case the external potential is too strong so almost no overtaking event occurs within the time interval $t = 5000t^*$.

VII. CONCLUSION

In recent experiments on rare sudden jump-like motion of particles along the director was observed with a jump length distribution that biased toward a half or a full particle length.[23] We put forward that these events may represent two types of particle motion, one in which particles overtake each other in the same column and the other where particles in a column re-equilibrate after a particle leaves the column.

To test this, we performed Brownian dynamics simulations of a quasi-one dimensional system of flexible, semi-flexible, or rigid particles to which a Gaussian confinement potential is applied. This potential mimics the effects of the self-consistent molecular field in the columnar phase. Our simulation results show that it is only in sufficiently small systems with reflecting boundary conditions and sufficiently large linear fractions that overtaking events present themselves as full jumps. This is mainly because in such systems the background fluctuations in the motion of particles are suppressed by the reflecting boundaries and small system size.

We also find that by increasing the linear fraction of particles or decreasing the system size the peaks in the self part of the Van Hove function become sharper, which means that the frequency of overtaking events not washed out by the background fluctuations increases. Moreover, we find a relation between time scale of the re-equilibration of a column after removing a particle from it and the self-diffusion time scale. This relation describes the results of our simulations accurately, confirming that at high linear fractions the re-equilibration process is much faster than the self-diffusion time scale.

We also considered the effect of particle bending flexibility on the overtaking events. We find that for flexible particles the background fluctuations are bigger and the effect of overtaking events is washed out by these fluctuations. As the flexibility decreases the amplitude of these fluctuations becomes smaller and overtaking events present themselves again as full jumps.

ACKNOWLEDGMENTS

The authors would like to thank S. Belli for providing the strength of the confining potential obtained from their simulations and Professor R. van Roij for the argument that explains the dependence of the time to fill a gap in a Tonks gas to the linear fraction of particles. We are grateful to E. Grelet and P. Lettinga for the trace of fd virus particles in the columnar phase. The work of S.N. forms part of the research program of the Dutch Polymer Institute (DPI, Project No. 698).

[1]Z. Dogic and S. Fraden, Curr. Opin. Colloid Interface Sci. **11**, 47 (2006).
[2]D. Frenkel and B. M. Mulder, Mol. Phys. **55**, 1171 (1985).
[3]D. Frenkel, H. N. W. Lekkerkerker, and A. Stroobants, Nature (London) **332**, 822 (1988).
[4]W. M. Gelbart, A. Ben-Shaul, and D. Roux, *Micelles, Membranes, Microemulsions, and Monolayers* (Springer, New York, 1994).
[5]L. Morales-Anda, H. H. Wensink, A. Galindo, and A. Gil-Villegas, J. Chem. Phys. **136**, 034901 (2012).
[6]F. M. van der Kooij and H. N. W. Lekkerkerker, J. Phys. Chem. B **102**, 7829 (1998).
[7]M. Baus, L. Rull, and J. P. Rykaert, *Observation, Prediction and Simulation of Phase Transitions in Complex Fluids* (Kluwer Academic Publishers, Dordrecht, 1995).
[8]Z. Dogic and S. Fraden, Phys. Rev. Lett. **78**, 2417 (1997).
[9]A. Kuijk, A. van Blaaderen, and A. Imhof, J. Am. Chem. Soc. **133**, 2346 (2011).
[10]L. Onsager, Ann. N.Y. Acad. Sci. **51**, 627 (1949).
[11]J. K. G. Dhont, *An Introduction to Dynamics of Colloids* (Elsevier Science, Amsterdam, 1996).
[12]M. Lettinga, E. Barry, and Z. Dogic, Europhys. Lett. **71**, 692 (2005).

[13]M. Bier, R. van Roij, M. Dijkstra, and P. van der Schoot, Phys. Rev. Lett. **101**, 215901 (2008).
[14]E. Grelet, M. P. Lettinga, M. Bier, R. van Roij, and P. van der Schoot, J. Phys.: Condens. Matter **20**, 494213 (2008).
[15]J. Kas, H. Strey, and E. Sackmann, Nature (London) **368**, 226 (1994).
[16]M. Lettinga and E. Grelet, Phys. Rev. Lett. **99**, 197802 (2007).
[17]E. Pouget, E. Grelet, and M. P. Lettinga, Phys. Rev. E **84**, 041704 (2011).
[18]E. Grelet, Phys. Rev. Lett. **100**, 168301 (2008).
[19]S. Dvinskikh, I. Furó, H. Zimmermann, and A. Maliniak, Phys. Rev. E **65**, 061701 (2002).
[20]R. Matena, M. Dijkstra, and A. Patti, Phys. Rev. E **81**, 021704 (2010).
[21]A. Patti, D. El Masri, R. van Roij, and M. Dijkstra, Phys. Rev. Lett. **103**, 248304 (2009).
[22]A. Patti, D. El Masri, R. van Roij, and M. Dijkstra, J. Chem. Phys. **132**, 224907 (2010).
[23]S. Naderi, E. Pouget, P. Ballesta, P. van der Schoot, M. P. Lettinga, and E. Grelet, Phys. Rev. Lett. **111**, 037801 (2013).
[24]Data are kindly provided by E. Grelet (CRPP, Bordeaux) and M. P. Lettinga (FZ Jülich) (unpublished).
[25]S. Belli, A. Patti, R. van Roij, and M. Dijkstra, J. Chem. Phys. **133**, 154514 (2010).
[26]A. Khokhlov and A. Semenov, Physica A **108**, 546 (1981).
[27]A. Khokhlov and A. Semenov, Physica A **112**, 605 (1982).
[28]T. Odijk, Macromolecules **16**, 1340 (1983).
[29]Data are kindly provided by S. Belli (Utrecht University).
[30]S. Plimpton, J. Comput. Phys. **117**, 1 (1995).
[31]M. Doi and S. Edwards, *The Theory of Polymer Dynamics* (Oxford University Press, USA, 1988), Vol. 73.
[32]L. Van Hove, Phys. Rev. **95**, 249 (1954).
[33]J. Hansen and I. McDonald, *Theory of Simple Liquids* (Academic Press, 2006).
[34]W. Kegel and A. van Blaaderen, Science **287**, 290 (2000).
[35]J. Barrat and J. Roux, J. Non-Cryst. Solids **131–133**, 255 (1991).
[36]B. Laird, J. McCoy, and A. Haymet, J. Chem. Phys. **87**, 5449 (1987).
[37]J. Percus, Phys. Rev. Lett. **8**, 462 (1962).
[38]Z. Salsburg, R. Zwanzig, and J. Kirkwood, J. Chem. Phys. **21**, 1098 (1953).
[39]H. van Beijeren, K. Kehr, and R. Kutner, Phys. Rev. B **28**, 5711 (1983).
[40]L. Lizana and T. Ambjörnsson, Phys. Rev. Lett. **100**, 200601 (2008).
[41]D. Levitt, J. Stat. Phys. **7**, 329 (1973).
[42]M. Kollmann, Phys. Rev. Lett. **90**, 180602 (2003).
[43]B. Lin, M. Meron, B. Cui, S. Rice, and H. Diamant, Phys. Rev. Lett. **94**, 216001 (2005).
[44]R. Kutner, H. Van Beijeren, and K. Kehr, Phys. Rev. B **30**, 4382 (1984).
[45]K. Mon and J. Percus, J. Chem. Phys. **117**, 2289 (2002).
[46]See supplementary material at http://dx.doi.org/10.1063/1.4823736 for the average distance between neighbors of a removed particle as a function of time.
[47]R. van Roij, personal communication (2010).
[48]L. Tonks, Phys. Rev. **50**, 955 (1936).
[49]P. van der Schoot, J. Phys. II France **6**, 1557 (1996).